Journal of Materials Chemistry B

Accepted Manuscript

ROYAL SOCIETY OF CHEMISTRY

www.rsc.org/materialsB

Journal of Materials Chemistry B RSCPublishing

PAPER

A delocalizable cationic headgroup together with an oligo-oxyethylene spacer in gemini cationic lipids improves their biological activity as vectors of plasmid DNA†

Cite this: DOI:

Received

DOI:

www.rsc.org/

Krishan Kumar,[a#] Ana L. Barrán-Berdón,[b#] Sougata Datta,[a#] Mónica Muñoz-Úbeda,[b] Clara Aicart-Ramos,[c] Paturu Kondaiah,[d] Elena Junquera,[b] Santanu Bhattacharya,*[a] and Emilio Aicart,*[b]

Lipoplex nano-aggregates constituted by plasmid DNA (pDNA) pEGFP-C3 and mixed cationic liposomes, consisting of several percentages of a gemini cationic lipid (GCL) of the 1,2-bis(hexadecyl imidazolium) oxyethylene series, referred as $(C_{16}Im)_2(C_2O)_n$, with oxyethylene spacers (n = 1, 2 or 3) between the imidazolium cationic groups, and the DOPE zwitterionic helper lipid, have been characterized by various biophysical and biological approaches carried out at several GCL compositions (α), and either the mass or the effective charge ratios of the lipoplex. The electrochemical study by ζ-potential confirms that the three GCLs yield a 10% lower effective charge than its nominal one, while compacted pDNA yields only a 25% effective negative charge. SAXS study reveals, irrespective of the spacer length (n) and effective charge ratio (ρ_{eff}), the presence of two lamellar structures, *i.e.*, the one ($L_{\alpha,\ main}$) in the whole GCL composition, and another ($L_{\alpha\ DOPE\ rich}$) with higher periodicity values that coexists with the previous one at low GCL composition ($\alpha = 0.2$). The cryo-TEM analysis shows two types of multilamellar structures consisting of cationic lipidic bilayers with pDNA sandwiched between them: a cluster-type (C-type) at low $\alpha = 0.2$, and a fingerprint-type (FP-type) at $\alpha \geq 0.5$, both with similar interlamellar spacing (d) in agreement to the $L_{\alpha,\ main}$ structure determined by SAXS. Transfection efficacies (TE) of each lipid mixture were determined in four different cell lines (HEK293T, HeLa, Caco-2 and A549) at several α and ρ_{eff} values in the absence and presence of serum (FBS). The optimized formulations ($\alpha = 0.2$ and $\rho_{eff} = 2.0$) substantially transfect cells much better than a commercial transfection reagent, Lipofectamine 2000 and previously studied efficient lipoplexes containing other cationic head groups or spacers both in the absence and presence of serum. The activity of optimized formulations may be attributed to the combination of several factors, such as: (a) the fusogenic character of DOPE which results in the higher fluidity of the lipoplexes at α = 0.2, (b) the coexistence of two lamellar structures at $\alpha = 0.2$ that synergizes the TE of these lipid vectors, and mainly (c) the higher biocompatibility of the GCLs reported in this work due the presence of two imidazolium cationic groups together with an oligo-oxyethylene spacer. The length of the spacer in the GCL seems to have less impact, although $(C_{16}Im)_2(C_2O)n$/DOPE-pDNA lipoplexes with n = 1 and 3 show relatively higher gene transfection than n = 2. All the optimum formulations reported herein are all highly efficient with negligible levels of toxicity, and thus, may be considered as very promising gene vectors for *in vivo* applications.

1. Introduction

Cationic lipids (CLs) are among the most promising carriers in gene therapy because they are able to efficiently compact the negatively charged DNA molecules.[1-6] They present several advantages over other non-viral vectors and, facilitate the cellular uptake due to their similarity with the cell membrane. However, when compared to viral vectors, CLs show lower transfection efficiency and some degree of cytotoxicity.[2,7-12] It is well-known that the molecular structure of the cationic lipids plays an important role in their interaction with nucleic acids as well as on the self-assembly of the lipoplexes. In order to look for efficient liposomal carriers, the design and

development of new cationic lipids is on the rise.[6,8,13-15] The continued efforts towards developing new lipids with improved properties, the gemini cationic lipids (GCLs) that are amphiphilic molecules containing two head groups linked by a rigid or flexible spacer, have appeared as prominent liposomal carriers for excellent gene transfections. These gemini lipids are promising candidates for successful gene therapy.[16-29] The molecular structure of GCLs provides an alternative way to develop new lipidic systems of practical relevance while offering a wide variety of structural modifications which may help to improve the transfection levels together with a better biocompatibility.[21,28-31] Such endeavours which can provide desirable outcomes include previous studies that have shown how the kind of polar headgroups, type of spacer and/or the hydrophobic chain length play an important role in the transfection process.[21-23,25,29,32-35] The crucial outcomes of the earlier studies have revealed that (a) the imidazolium based headgroups in cationic lipids have emerged as an interesting tool which gives rise to systems with excellent gene transfection capability even better than their ammonium head group counterparts,[23,34,36] (b) the short spacer length between the head groups results in a higher transfection efficiency;[23-25] and (c) the presence of a hydrophilic spacer (oligo-oxyethylene) in to the gemini lipid structure so as to optimize the interaction of the lipid vector with the nucleic acid.[22] Accordingly, the combination of imidazolium based headgroups and oligo-oxyethylene-type spacer in the GCL structure may provide potentially effective carriers of plasmid DNA.

Following these guidelines, in order to improve the desirability of CLs as biocompatible gene delivery vectors, this work reports a study with lipoplexes based on a new type of GCLs containing two imidazolium cationic headgroups, two C_{16} hydrophobic tails, and short oligo-oxyethylene spacers. The lipoplexes are formed by pEGFP-C3 plasmid DNA (pDNA) and mixed liposomes containing a GCL of the bis(hexadecyl imidazolium) oxyethylene series, referred as $(C_{16}Im)_2(C_2O)_n$, where n (= 1, 2 or 3) is the length of the oxyethylene spacer between the imidazolium headgroups (see Scheme 1) and DOPE (a zwitterionic helper lipid). The use of a hydrophilic spacer together with the imidazolium headgroups may provide a better lipid-DNA interaction and improved transfection capabilities compared with the GCLs series reported earlier. The transfection efficacies were checked out in four different cell lines *in vitro* by flow cytometry (FACS), fluorescence and confocal microscopy. The cell viabilities/cytotoxicity were determined by MTT assays. The extensive biophysical and biochemical characterizations were carried out on lipoplexes in order to correlate with their transfection efficacies. The referred lipoplexes have been analyzed by the measurements of ζ-potential, SAXS, cryo-TEM, and fluorescence anisotropy. Taken together, we demonstrate that the co-liposomes of these gemini cationic lipids with DOPE transfect pDNA in to cell lines of different origins efficiently and give rise to remarkably high gene expression levels both in the absence and presence of serum (FBS) as well as deal with toxicity profile of lipids significantly.

2. Experimental

2.1. Materials

The pEGFP-C3 Plasmid DNA (pDNA) was extracted from competent *E. Coli* bacteria previously transformed with pEGFP-C3, the extraction being carried out using GenElute HP Select plasmid Gigaprep Kit (Sigma Aldrich) following a protocol previously described.[23,25] Sodium salt of calf thymus DNA (ctDNA), provided by Sigma-Aldrich, was used as linear DNA to determine the lipid charge ($q^+_{L^+}$) of the GCL. The zwitterionic lipid, 1,2-dioleoyl-*sn*-*glycero*-3-phosphatidylethanolamine (DOPE) was purchased from Avanti Polar Lipids. The divalent cationic gemini lipids of the bis(hexadecyl dimethyl imidazolium) oxyethylene series, referred to as $(C_{16}Im)_2(C_2O)_n$, with the polyoxyethylene spacer n = 1, 2 or 3, were synthesized according to the procedure described in Scheme 1.

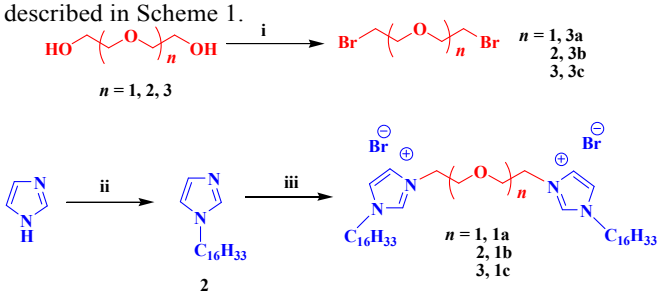

Scheme 1 The synthetic route of the gemini cationic lipid [bis(hexadecyl dimethyl imidazolium) oxyethylene] series (**1a-c**), referred to as $(C_{16}Im)_2(C_2O)_n$, where n = 1, 2, or 3. (i) PBr_3, 50-60 °C, 12 h, yield ~80% (n = 1), 85% (n = 2), 90% (n = 3); (ii) $C_{16}H_{33}Br$, K_2CO_3, KI, dry acetone, 70 °C, 12 h, ~80%; (iii) $BrCH_2(CH_2OCH_2)_nCH_2Br$, dry ethanol, sealed tube, 80 °C, 72 h, ~80% (n = 1), 82% (n = 2), 85% (n = 3).

2.2. Synthesis of the Bis(hexadecyl dimethyl imidazolium) oxyethylene surfactants

All the reagents and solvents used for the present study were of highest grade available commercially. The solvents used were dried properly. Imidazole, *n*-hexadecyl bromide, PBr_3 and diols were bought from Aldrich chemical company. Each synthesized compound was characterized by ^{1}H-NMR spectra recorded in $CDCl_3$ in Bruker 400 MHz NMR spectrometer. Chemical shifts (δ) are reported in ppm downfield from the internal standard (TMS). Elemental analysis was recorded in Thermo Finnigan EA FLASH 1112 SERIES.

2.2.1. Synthesis of dibromides (3a-c) and *N*-*n*-hexadecyl imidazole (2). The dibromides (**3a-c**) and *N*-*n*-hexadecyl imidazole (**2**) were synthesized as described in the reported procedure.[22,35,37]

2.2.2. Synthesis of Bis(quaternary imidazolium) surfactants (1a-d). The bis(quaternary imidazolium) surfactants were synthesized as described in the previous reports.[35,38] All the surfactants (**1a-d**) were obtained by refluxing the corresponding α,ω-dibromoalkoxyalkanes (1.315 mmol) with *N*-*n*-hexadecyl imidazole (3.947 mmol) in dry ethanol at ~80 °C for 72 h. After that the ethanol was completely removed under vacuum from the reaction mixture, the solid obtained was dissolved in minimum volume of methanol and precipitated several times by drop wise addition in ethyl acetate. The purity of the solid surfactants was determined from ^{1}H-NMR spectra and elemental analysis. The overall yields of the surfactants ranged from 80-85%.

2.2.3. Bis(hexadecylimidazolium)diethyl ether (1a). ^{1}H-NMR ($CDCl_3$, 400 MHz, TMS, rt) : δ 0.88 (t, 6H), 1.25-1.33 (s + br m, 52H), 1.89-1.90 (m, 4H), 3.99 (t, 4H), 4.38 (t, 4H), 4.66 (t, 4H), 7.25 (s, 2H), 8.06 (s, 2H), 10.34 (s, 2H); ESI-MS: m/z 328.30 $[M]^{2+}$, calcd. for $[C_{42}H_{80}N_4O]^{2+}$; Elemental analysis calcd. for $C_{42}H_{80}N_4OBr_2$: C 61.75, H 9.87, N 6.86; found C 61.70, H 9.85, N 6.90.

2.2.4. Bis(hexadecylimidazolium)diethoxyethane (1b). ^{1}H-NMR ($CDCl_3$, 400 MHz, TMS, rt) : δ 0.88 (t, 6H), 1.25-1.33 (s

+ br m, 52H), 1.91 (t, 4H), 3.67 (s, 4H), 3.95 (t, 4H), 4.34 (t, 4H), 4.62 (t, 4H), 7.47 (s, 2H), 7.75 (s, 2H), 10.12 (s, 2H); ESI-MS: m/z 350.33 $[M]^{2+}$, calcd. for $[C_{44}H_{84}N_4O_2]^{2+}$; Elemental analysis calcd. for $C_{44}H_{84}N_4O_2Br_2$, H_2O: C 60.12, H 9.86, N 6.37; found C 60.10, H 9.83, N 6.40.

2.2.5. Bis(hexadecylimidazolium)bis(ethoxyethyl)ether (1c). ^{1}H-NMR ($CDCl_3$, 400 MHz, TMS, rt) : δ 0.86 (t, 6H), 1.23-1.31 (s + br m, 52H), 1.88-1.90 (br s, 4H), 3.61 (s, 4H), 3.68 (s, 4H), 3.97 (s, 4H), 4.31 (t, 4H), 4.64 (t, 4H), 7.49 (s, 2H), 7.73 (s, 2H), 10.19 (s, 2H); ESI-MS: m/z 372.34 $[M]^{2+}$, calcd. for $[C_{46}H_{88}N_4O_3]^{2+}$; Elemental analysis calcd. for $C_{46}H_{88}N_4O_3Br_2$: C 61.05, H 9.80, N 6.19; found C 61.09, H 9.82, N 6.15.

2.3. Characterization of lipoplexes

The films of mixed lipids were prepared by dissolving appropriate amounts of gemini cationic lipid (L^+) and DOPE (L^0) in chloroform to obtain the desired molar fraction composition (α) of the GCL in the mixed liposome. Afterwards, chloroform was removed under high vacuum to yield a dry lipid film that was finally hydrated with HEPES buffer (40 mM, pH = 7.4) and sequentially extruded according to a procedure previously described.[23,25] The desired lipoplex composition, either in terms of the mass ratio (L/D), between total lipid ($L = L^+ + L^0$) to plasmid DNA (D), or the effective charge ratio (ρ_{eff}), between the GCL and pDNA charges, was obtained by mixing equal volumes of pDNA and $(C_{16}Am)_2(C_2O)_n$ liposomal suspensions.[39] The concentrations of pDNA, to fit the optimum conditions for each experimental technique, were used as follows: 0.05 mg/mL for zeta potential and fluorescence anisotropy, 1 mg/mL for cryo-TEM, 200 µg/capillary for SAXS, 0.8 µg/well (24 well cell culture plate) for TE determination and 0.2 µg/well (96 well cell culture plate) for the cell viability assays.

Size and ζ-potential measurements were made, at 25 ºC, with a Phase Analysis Light Scattering technique (Zeta PALS, Brookhaven Instrum. Corp., USA).[24,25] Each electrophoretic mobility datum was taken as an average over 50 independent measurements. ζ-potential for the lipoplexes was measured at different GCL compositions (α) of the mixed lipid, and at several L/D ratios of the lipoplexes.

Small-angle X-ray scattering (SAXS) experiments were performed at the BM26 at European Synchrotron Radiation Facility (ESRF) Grenoble (France). The energy of the incident beam was 12.6 KeV (λ = 0.995 Å). Samples were placed in sealed glass capillaries from Hilgenberg with an outside diameter of 1.5 mm. SAXS experiments were run, at each α, and at several effective charge ratios (ρ_{eff}) of the lipoplexes.[25]

Cryo-TEM experiments were prepared following the standard procedures.[40,41] In these experiments, perforated Quantifoil R1.2/1.3 (hole diameter 1.2 µm) on a 400-mesh copper grid were used. Images were obtained using a Jeol JEM 2011 cryo-electron microscope operated at 200 kV, under low-dose conditions, and using different degrees of defocus (500–700 nm) to obtain an adequate phase contrast.[42] Images were recorded on a Gatan 794 Multiscan digital camera. These CCD images were processed and analyzed with a Digital Micrograph.

Fluorescence anisotropy of 1,6-diphenylhexatriene (DPH) probe was determined with a Perkin Elmer LS-50B Luminiscence Spectrometer by measuring the intensities of the polarized light emitted by DPH, as described previously.[43] DPH included in the liposomal membrane was excited at 360 nm and its fluorescence emission was recorded at 430 nm, with a slit width of 2.5 nm for both the excitation and the emission.

Transfection of pEGFP-C3 plasmid DNA (pDNA, 0.8 µg) across HEK293T (Human embryo kidney, transformed), HeLa (Human cervical cell carcinoma), Caco-2 (Human epithelial colorectal adenocarcinoma), and A549 (Adenocarcinomic human alveolar basal epithelial) cells using $(C_{16}Im)_2(C_2O)_n$/DOPE lipid mixtures was performed in absence (-FBS) and presence (+FBS) of serum, as fully described previously.[23,25] Transfection efficacies (GFP expression) were analyzed 48 h post transfection using Flow Assisted Cell Sorting (FACS). Data obtained from FACS were analyzed using public domain software WinMDI 2.9. Results were plotted as % GFP positive cells and mean fluorescence intensity (MFI) against the effective charge ratio (ρ_{eff}) on GraphPad Prism 5.0 software. Lipofectamine 2000 was used as a positive control in all the transfection experiments and acronymed as Lipo2000 and Lipo2000* for absence of serum (-FBS) and presence of serum (+FBS) conditions respectively.[25]

To observe the GFP expression, fluorescence microscopy was performed on IX81 Olympus fluorescence microscope 48 h post transfection.

Confocal microscopy study was also performed to visualize the Cy-5 labeled pDNA internalization in transfected cells after 6 h of incubation (Zeiss LSM 510-Meta Apochromat). Cells were transfected as mentioned above using optimized lipoplex formulations in presence of serum (+FBS) conditions while Lipo2000* was used as a positive control.

The cell viability data were obtained by performing using 3-(4,5-dimethylthiazole-2-yl)-2,5-diphenyl tetrazolium bromide reduction method (MTT assay) in the same cell lines used for the transfection studies.[19,44] Briefly, lipoplexes were incubated with cells following the actual transfection conditions and MTT was added at the end of the experiment to each well for 4 h. The entire medium was removed from wells and the formazan crystals that formed were dissolved in DMSO. The absorbance was measured using a microtiter plate reader at 570 nm and % cell viability was determined as detailed previously.

3. Results and discussion

When CLs are used as carriers of DNA molecules, several aspects must be evaluated. These include (a) compaction and protection of DNA by the gene vector, (b) electrostatic interaction between positive CL and negative DNA, and of the cationic lipoplex with the negative charged cell membrane, (c) internalization of the lipoplex in to the cells, and release of DNA in the cytoplasm, and (d) nuclear entrance of DNA for gene expression. Based on that, electrostatic interaction between CLs and DNA, together with the structure, size, morphology and fluidity of the lipoplexes certainly affect the cellular interaction and thus, a detailed lipoplex characterization in absence of cells (steps a-b) may help one to understand their behavior appropriately in the presence of cells (steps c-d).

3.1. Biophysics of the lipoplex nano-aggregates

In order to analyze the formation of the lipoplex between each GCL and DNA, several factors are important. Firstly, a high percentage of GCL and DNA counterions are expelled to the bulk, which results in a net entropy gain.[45] Secondly, a strong electrostatic interaction operates between positive GCLs and negative DNA. Based on these, the electrochemical properties of lipoplexes have been evaluated by measuring changes in ζ-potential. This is an appropriate tool because it permits the determination of the electroneutrality mass ratio and the effective charges of both, GCL and pDNA, when the lipoplex is formed. Fig. 1 (and Fig. S1 of the ESI) show changes in ζ-

potential results *vs* total lipid/DNA mass ratio (L/D) for the (($C_{16}Im)_2(C_2O)_n$/DOPE-pDNA) and (($C_{16}Im)_2(C_2O)_n$/DOPE-ctDNA) lipoplexes.

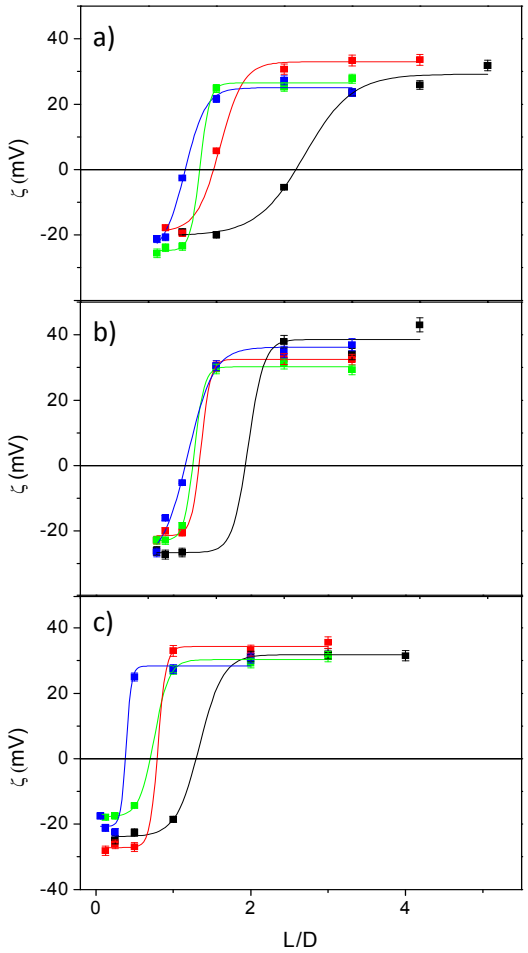

Fig. 1. Plots of ζ-potential *vs* lipoplex nano-aggregate composition (L/D) at several GCL composition (α): (a) $(C_{16}Im)_2(C_2O)$/DOPE-pDNA; (b) $(C_{16}Im)_2(C_2O)_2$/DOPE-pDNA; (c) $(C_{16}Im)_2(C_2O)_3$/ DOPE-pDNA. Errors are within ± 5%. In all plots: black, α = 0.2; red, α = 0.4; green, α = 0.5; and blue, α = 0.7.

These results clearly show the electroneutrality values $(L/D)_\phi$ for each lipoplex (see Table S1 of ESI) where the positive and negative charges are equal (ρ_{eff} = 1) and this quantity is the lower limit from which lipoplexes are potentially adequate to be used as transfecting vectors.[24] From the $(L/D)_\phi$ values (not reported) for the (($C_{16}Im)_2(C_2O)_n$/DOPE-ctDNA) lipoplexes following a procedure reported previously[22,23] and presented in the ESI, it has been possible to allow the effective GCL charge ($q^+_{L^+}$) for the three GCLs of this work. An average value of $q^+_{L^+}$ = 1.8 ± 0.1 was obtained for the three $(C_{16}Im)_2(C_2O)_n$/DOPE GCLs (see Table S1 of ESI) which is 10% lower than the nominal ones ($q^+_{L^+}$ = + 2). Once the effective charge ($q^+_{L^+}$) of the GCL is known, it is possible to determine the effective charge of pDNA (q^-_{pDNA}) from the $(L/D)_\phi$ values for $(C_{16}Im)_2(C_2O)_n$/DOPE-pDNA lipoplexes (see Table S1 for both, $q^+_{L^+}$ and q^-_{pDNA}). Fig. S2 reports q^-_{pDNA} *vs* the GCL composition (α). Similar to the observations reported earlier for the GCL/DOPE-pDNA lipoplexes, the q^-_{pDNA} values in this work are only ~25 % of the nominal charge of pDNA (-2 per bp). This confirms that when the lipoplex is formed, pDNA retains ~75% of Na^+ counterions. It should also be noted that q^-_{pDNA} remains roughly constant, irrespective of the spacer length of the GCL or the composition of the mixed liposome (α).[22,24,25,46] In order to prepare appropriate formulations for gene transfection, the lipoplexes must have a net positive charge even if it is small. The previous information provided by the ζ-potential measurements indicates that much less CL is required than the expected concentration to obtain positive lipoplexes with pDNA which results in a decrease of their toxicity significantly during their interaction with cells.

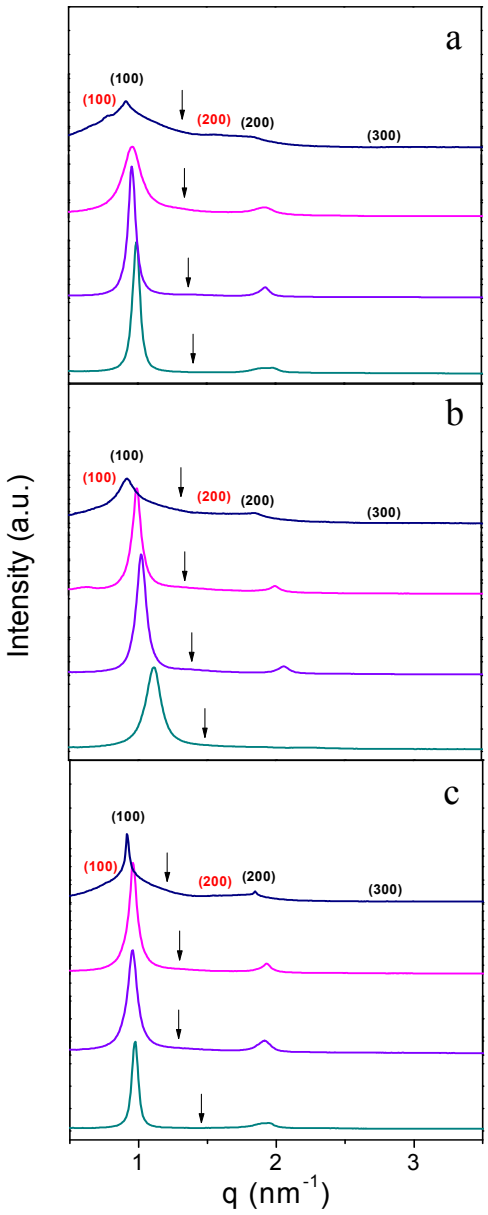

Fig. 2 SAXS diffractograms of $(C_{16}Im)_2(C_2O)_n$/DOPE-pDNA lipoplexes at various GCL compositions (α) and effective charge ratio (ρ_{eff}) = 1.5. (a) n = 1, (b) n = 2, and (c) n = 3. Black lines, α = 0.2; pink lines, α = 0.4; blue lines, α = 0.5; and green lines, α = 0.7. Miller indices (hkl) correspond to the lamellar structures: red, $L_{\alpha,DOPE\ rich}$; and black, $L_{\alpha\ main}$. Arrows indicate the pDNA-pDNA correlation peak.

The size, structure, morphology and fluidity of lipoplexes affect their gene transfection capabilities. The lipoplex characteristics have been analyzed by means of PALS, SAXS, cryo-TEM and fluorescence anisotropy. The particle size was measured for the three mixed liposomes, $(C_{16}Im)_2(C_2O)_n$/DOPE with n = 1, 2 or 3, the average sizes, in nm, were roughly independent on n, but decreased in comparison to the composition of the mixed liposome (α) as (108 ± 2); (106 ± 4); (97 ± 9), and (86 ± 7) at α = 0.2, 0.4, 0.5 and 0.7, respectively. Though, the same hydration and extrusion procedure[47] was maintained for all the samples, the slight decrease in the size with α may be due to the different aggregation properties of the GCLs in presence of the helper lipid, DOPE.[48,49]

The structure of the $(C_{16}Im)_2(C_2O)_n$/DOPE-pDNA lipoplexes were determined from SAXS experiments in concentrated samples, at several mixed lipid compositions (α) and at various effective charge ratios ($\rho_{eff} > 1$) where lipoplexes are potentially active as gene transfection vectors. SAXS diffractograms (Fig. 2) show Intensity *vs* q factor, for ρ_{eff} = 1.5 at several α values for the three $(C_{16}Im)_2(C_2O)_n$/DOPE-pDNA lipoplexes (see Figs. S3-S5 of ESI for the remaining ρ_{eff} = 2.0; 2.5, and 3.0). The correlation of Bragg peaks indicates that, in all the cases irrespective of α or ρ_{eff}, lipoplexes form a lamellar structure ($L_{\alpha\ main}$) represented by alternating layers of mixed lipids (GCL + DOPE helper lipid) and pDNA helices, where d (= $d_m + d_w$) is the sum of the thicknesses of the lipid bilayer (d_m) and the coiled pDNA aqueous monolayer (d_w) and also related to the q factor of first peak ($d = 2\pi/q_{100}$). All diffractograms show an intermediate broad peak that is related to the pDNA-pDNA correlation (marked with arrows) which permits to get the distance d_{pDNA} between DNA helices within this monolayer ($d_{pDNA} = 2\pi/q_{pDNA}$). Additionally, diffractograms of mixed lipid composition at α = 0.2 (the lowest GCL and richest DOPE composition) at all the ρ_{eff} charge ratios show that the peaks of the lamellar structure are broad and apparently asymmetric which suggest the presence of an additional structure with not much different parameters. Deconvolution of these two peaks in all diffractograms at α = 0.2 have confirmed the presence in an additional lamellar structure ($L_{\alpha\ DOPE\ rich}$) at slightly lower q factor, and thus with higher periodicity (d). Tables S2-S4 of ESI report all the parameters for both structures.

Fig. 3 and Fig. S6 (a, b) of ESI report the values of the periodic distance (d), and the d_{pDNA} for the main lamellar structure, as a function of α, at all effective charge ratios (ρ_{eff}) for the three lipoplexes of this work. It is shown that, in all cases, values of d and d_{pDNA} obtained for the $L_{\alpha\ main}$ structure of the $(C_{16}Im)_2(C_2O)_n$/DOPE-pDNA lipoplexes remain independent of ρ_{eff}, while a decrease with α was found for: *i*) the periodicity d in the range 6.7-5.7 nm, and *ii*) the d_{pDNA} values in the range 4.5-5.0 nm. This decrease in both parameters, clearer for lipoplexes containing GCL with longer spacer (n = 2 or 3), is similar to what was reported for lipoplexes of other CLs with different headgroups or spacers.[25,50,51] This may be attributed to the combination of the facts that a thinner bilayer (d_m) with increasing α because the length of the GCLs is slightly shorter than that of DOPE, and a decrease of the pDNA aqueous monolayer (d_w) and of d_{pDNA} as the GCL content increases, resulting in a higher pDNA compaction. In any case, the d values, together d_m ~ 4.0-4.5 nm, assumed for the lipid bilayer from the molecular structures of GCLs and DOPE, permit an estimation of the thickness of the monolayer (d_w ~ 2.0-2.5 nm) to allocate the plasmid DNA. It should be noted that, at α = 0.2, the other $L_{\alpha\ DOPE\ rich}$ lamellar structure with less GCL content, that coexists with the $L_{\alpha\ main}$ one, is less compact and thus has a higher periodicity in d values ranging from 7.9 to 9.4 nm (see Tables S2-S4 of ESI).

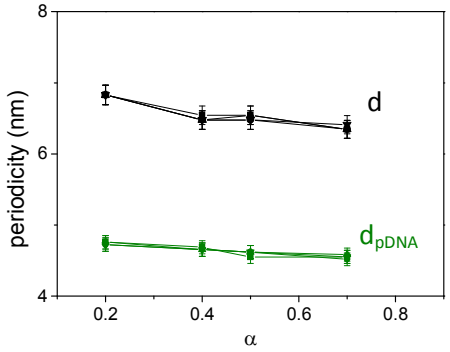

Fig. 3 Plots of the periodic distance of the main lamellar structure (d) and the pDNA-pDNA correlation (d_{pDNA}) for $(C_{16}Im)_2(C_2O)$/DOPE-pDNA lipoplexes *vs* GCL composition (α) at several effective charge ratios (ρ_{eff}). Squares, ρ_{eff} = 1.5; circles, ρ_{eff} = 2.0; up triangles, ρ_{eff} = 2.5; and down triangles, ρ_{eff} = 3.0.

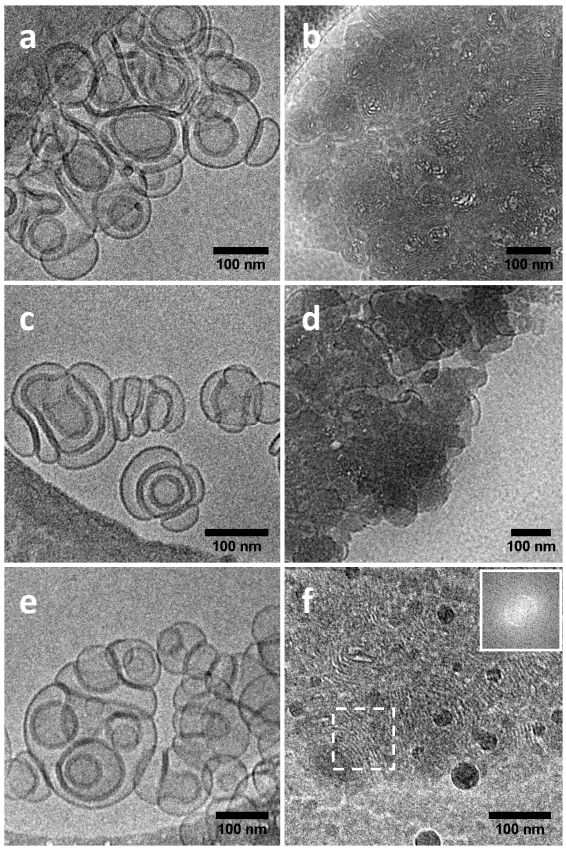

Fig. 4 A selection of cryo-TEM micrographs showing a general view of the $(C_{16}Im)_2(C_2O)_1$/DOPE-pDNA lipoplex nano-aggregates at two GCL compositions (α). $(C_{16}Im)_2(C_2O)_1$/DOPE-pDNA at α = 0.2 (a), and α = 0.5 (b); $(C_{16}Im)_2(C_2O)_2$/DOPE-pDNA at α = 0.2 (c), and α = 0.5 (d); $(C_{16}Im)_2(C_2O)_3$/DOPE-pDNA at α = 0.2 (e), and α = 0.5 (f).

Cryo-TEM experiments, that are reported to characterize the size, shape, and morphology of a wide variety of lipoplexes,[22,23,25,46,52] were performed on positive $(C_{16}Im)_2(C_2O)_n$/DOPE-pDNA (n = 1, 2 and 3) lipoplexes at two

GCL compositions, α = 0.2 and 0.5. Micrographs reported in Fig. 4 (and others not shown) reveal the presence of lipoplexes characterized by a multilamellar arrangement, with two different types of nano-aggregates depending on α, a behavior already found in the lipoplexes with GCLs containing imidazolium headgroups or an oligo-oxyethylene spacer.[22,23,25] Thus, at higher DOPE content (α = 0.2), pDNA induces a typical aggregation by disrupting some liposomes that form few multilayers surrounding the other organized liposomes (with pDNA sandwiched in between) which results in the formation of cluster-type nanostructures (C-type) in all GCLs (with n = 1, 2 and 3). However, when the GCL content of the mixed liposomes increases (α = 0.5) most of the liposomes are disrupted, and lipoplexes present a fingerprint pattern (FP-type) with a continuous multilamellae, also documented in the literature.[22,23,50,53-55] These FP-type nanostructure is clearer for $(C_{16}Im)_2(C_2O)$/DOPE-pDNA and $(C_{16}Im)_2(C_2O)_3$/DOPE-pDNA lipoplexes (with n = 1 or 3) while for $(C_{16}Im)_2(C_2O)_2$/DOPE-pDNA lipoplexes (with n = 2) both C-type and FP-type nanostructures are coexisting. According to these observations the GCLs favor the appearance of FP-type nano-aggregates and some of them (and others not shown) are chosen to analyze the presence of a periodicity (Fig. 4). The inset of Fig. 4 shows, as an example, a Fast Fourier Transform (FFT) profile where the diffraction spot corresponds to a typical lamellar pattern. Similar values (6.6 ± 0.4 nm) and (6.4 ± 0.4 nm) were obtained for the interlamellar spacing (d) in both C and FP patterns (at α = 0.2 and 0.5), respectively. These values are in good agreement to those found from SAXS study for the $L_{\alpha\ main}$ structure, confirming the multilamellar structure.

Fluorescence anisotropy (r), a biophysical property that is related to the transfection activity of the liposomal gene delivery vector, was determined as a measurement of the bilayer fluidity of the $(C_{16}Im)_2(C_2O)_n$/DOPE-pDNA lipoplexes.[56-58] Conceptually, when a bilayer becomes more fluidic, the degree of rotation of an excited fluorescent probe placed within the same increases and its anisotropy decreases. Fig. S7 (a-f) of ESI shows the anisotropy values of the DPH fluorophore located in the bilayer of the $(C_{16}Im)_2(C_2O)_n$/DOPE liposomes, in the absence ($\rho_{eff} = \infty$) and presence of pDNA, as a function of temperature. Results in Fig. S7 reveal that, in all the cases, fluorescence anisotropy decreases with T which indicates that the fluidity of the lipid bilayer increases. Also due the presence of DOPE, the gel-to-fluid transition temperature (T_m) decreases, and the fluidity of lipoplexes increases with the increasing DOPE content (at α = 0.2).[56,59] Additionally, the very low anisotropy levels at physiological temperature (0.07-0.15) shown by the three $(C_{16}Im)_2(C_2O)_n$/DOPE-pDNA lipoplexes reported here present them as fluid nano-aggregates, that are potentially attractive as pDNA transfection vectors.

3.2. Biological activity of the lipoplexes

Gene transfection capability of mixed liposome formulations, $(C_{16}Im)_2(C_2O)_n$/DOPE with n = 1, 2 or 3, was investigated by performing transfections of a green fluorescence protein (GFP) expressing pEGFP-C3 plasmid DNA (pDNA) both in absence (-FBS) and presence of 10% serum (+FBS) under flow cytometry. The GFP expression due to transfection was analyzed in terms of the percentage GFP positive cells in transfected population (% GFP cells), and the mean fluorescence intensity (MFI) of GFP per cell. Herein, we studied four GCL compositions (α) of the lipid mixture (0.2, 0.4, 0.5 and 0.7) by undertaking five effective charge ratio of the lipoplex, ρ_{eff} (1.5, 2, 2.5, 3 and 5). The transfection performed in the absence of serum (-FBS) revealed that mixed liposomes of each of the three GCLs showed remarkably high GFP expression levels at all GCL compositions (Figs. S9-S11 of ESI). Among all the formulations, α = 0.2 appeared to have relatively higher gene transfection capability than other GCL compositions. The maximum gene expression levels (MFI ~500) observed were significantly higher than a commercial lipofection reagent, Lipo2000 (MFI ~200) that was used as a positive control (see Fig. 5 a, c and e).

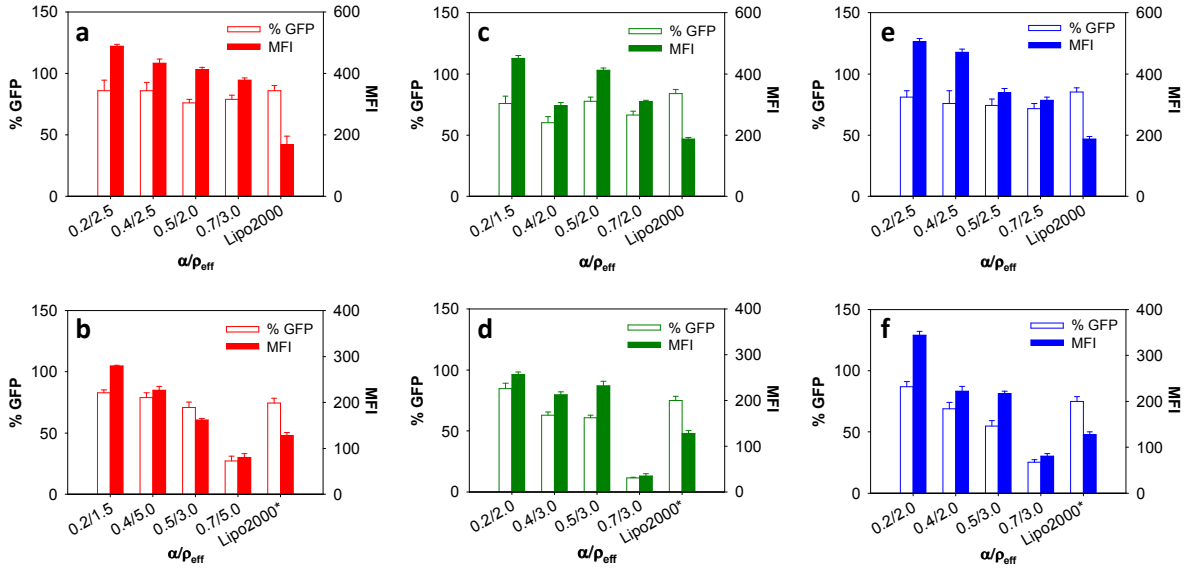

Fig. 5 Transfection of pEGFP-C3 DNA in HEK293T cells in the absence (-FBS) [a, c and e] and presence of serum (+FBS) [b, d and f] using lipoplexes of $(C_{16}Im)_2(C_2O)$/DOPE (a, b), $(C_{16}Im)_2(C_2O)_2$/DOPE (c, d) and $(C_{16}Im)_2(C_2O)_3$/DOPE (e, f) at α = 0.2, 0.4, 0.5 and 0.7, and ρ_{eff} = 1.5, 2, 2.5, 3.0 and 5 as mentioned in bar diagrams. Lipo2000 and Lipo2000* were used as positive controls for (-FBS) and (+FBS) transfections, respectively.

Subsequently, the GFP expression levels were also assessed for transfections in the presence of serum (+FBS). It is well-known that the presence of serum deteriorates the transfection efficacies mediated by cationic lipids. Thus the development of liposomal

systems producing desirable gene expression in the presence of serum are the essential prerequisites for gene therapy to be practically beneficial.[60,61] All the GCL formulations shown here could transfect cells substantially in the presence of serum (Fig. S12-S14 of ESI). Though, there was a little reduction in GFP expression levels (MFI) relative to transfections performed in the absence of serum, it was still significantly higher than Lipo2000* in the presence of serum. The Fig. 5 presents the optimum charge ratio of the lipoplex (ρ_{eff}) at each composition (α) for the three lipoplexes $(C_{16}Im)_2(C_2O)_n$/DOPE-pDNA with n = 1, 2 or 3, in the absence (a, c and e) and presence (b, d and f) of serum. The GCL formulations with α = 0.2 afforded maximum GFP expression levels relative to other GCL compositions. On the other hand, liposomal formulations with α = 0.4 and 0.5 were also efficient enough to transfect cells even better than Lipo2000*. Notably, an interesting phenomenon was observed for transfections in presence of serum where a sudden drastic decrease in GFP levels was observed for high GCL composition, (α = 0.7) even down to Lipo2000* (Fig. 5). Interestingly, a descending order of gene transfection capability was observed with ascending order of GCL molar composition (α). This phenomenon was quite consistent for all GCL formulations. It should also be noted here that the transfection efficacies of lipoplexes derived from different liposomal formulations with relatively lower GCL composition (α = 0.2) was better at lower ρ_{eff}. However, lipoplexes derived from liposomal formulations with higher GCL composition ($\alpha \geq 0.4$) showed high gene transfection efficiency at higher ρ_{eff}. Based on the FACS analysis (Fig. 5), it may be concluded that the overall trend of TE, in absence and presence of serum, was not influenced by the variation in spacer length between the cationic headgroups of the GCL. The maximum TE for each GCL was from the lipoplex of the optimized formulations (α = 0.2) in general and the best activity in the presence of serum was shown by each lipoplex of α = 0.2 at ρ_{eff} = 1.5 or 2.0.

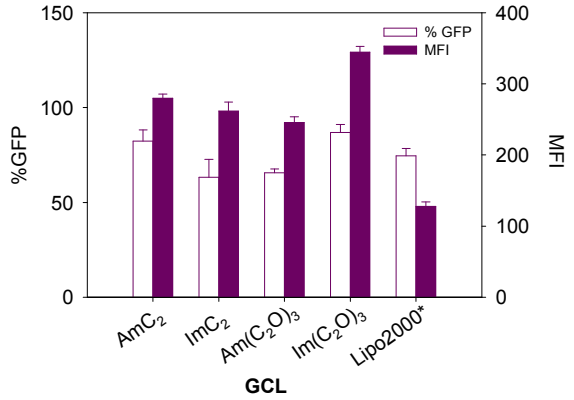

Fig. 6 Transfection of pEGFP-C3 DNA with lipoplexes for optimized formulations in HEK293T cells in the presence of serum (+FBS). $(C_{16}Am)_2C_2$/DOPE-pDNA referred as AmC_2; $(C_{16}Im)_2C_2$/DOPE-pDNA referred as ImC_2; $(C_{16}Am)_2(C_2O)_3$/DOPE-pDNA referred as $Am(C_2O)_3$, and; $(C_{16}Im)_2(C_2O)_3$/DOPE-pDNA referred as $Im(C_2O)_3$. Lipo2000* served as a positive control.

Earlier we have reported an extensive careful biophysical and biological characterization of the different series of lipoplexes formed by plasmid DNA and mixed lipids containing the DOPE helper lipid and different types of cationic gemini lipids, as follows: a) with bis(hexadecyl dimethyl ammonium) alkane, the series referred as $(C_{16}Am)_2C_n$/DOPE-pDNA where C_n is the alkyl spacer with n = 2, 3, 5 or 12;[24,25] b) with bis(hexadecyl imidazolium) alkane, the series $(C_{16}Im)_2C_n$/DOPE-pDNA with n = 2, 3, 5 or 12;[23] and c) with bis(hexadecyl dimethyl ammonium) oxyethylene, the series $(C_{16}Am)_2(C_2O)_n$ where $(C_2O)_n$ is the oligo-oxyethylene spacer with n = 1, 2 or 3.[22] Fig. 6 reports the TE obtained using the optimum formulations for each series together with that obtained for the series of the present work for comparison. Results show that, in the presence of serum, all the optimized formulations for each studied series are superior in terms of the transfection efficiency than the positive control Lipo2000* while $(C_{16}Im)_2(C_2O)_3$/DOPE-pDNA lipoplex reported in the present work is the one with highest transfection capability.

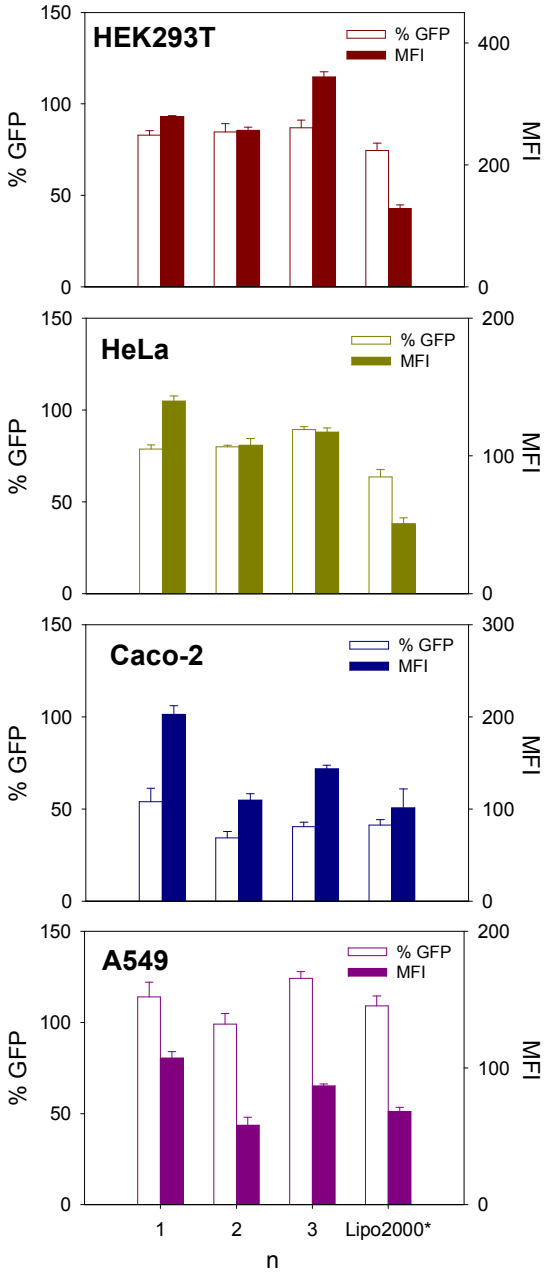

Fig. 7 Transfection of pEGFP-C3 DNA with lipoplexes of $(C_{16}Im)_2(C_2O)_n$/DOPE-pDNA with n = 1, 2 and 3, for optimized formulation (α = 0.2 at ρ_{eff} = 2.0) in HEK293T, HeLa, Caco-2, and A549 cells, in the presence of serum (+FBS). Lipo2000* served as a positive control.

The TE of all the optimized GCL compositions (α = 0.2) for the three $(C_{16}Im)_2(C_2O)_n$/DOPE-pDNA lipoplexes were also checked out in three other cell lines (HeLa, Caco-2 and A549) and the results are reported in Fig. 7. All the optimized formulations showed excellent gene transfection capability in all the cell lines which were

also significantly higher than Lipo2000*. The $(C_{16}Im)_2(C_2O)_n$/DOPE-pDNA lipoplexes (with n = 1 and 3) showed similar and relatively higher GFP expression than the other optimum formulation (with n = 2). Thus, it could be emphasized here that, irrespective of the number of oxyethylene units of the spacer region between the two cationic imidazolium groups of the GCL, all mixed liposome formulations reported in this work are efficient enough to transfect cell lines of different origins in a significant approach and are promising candidates for practical *in vivo* applications.

The GFP expressions originated due to different transfections mediated by efficient formulations in the presence of serum were also viewed under a fluorescence microscope. Fig. 8 and Fig. S15 of ESI, reporting the observed GFP expressions in HEK293T, Caco-2 and HeLa cells, confirm the flow cytometry analysis discussed above. The cells transfected with lipoplexes (at α = 0.2 and ρ_{eff} = 2.0) of all the $(C_{16}Im)_2(C_2O)_n$/DOPE formulations revealed higher GFP expression being more prominent than that of Lipo2000* transfections.

The gene expression levels were also corroborated based on pDNA cellular transfection studies where Cy-5 labeled pDNA was used for lipoplex preparation and the resulting lipoplexes were incubated with cells in the presence of serum (+FBS). The transfection samples were viewed under a confocal microscope and it revealed an efficient internalization of pDNA molecules (Fig. 9). The pDNA fluorescence in the cells transfected with GCL optimized formulations was significantly higher than those of Lipo2000* treated cells. The labeled pDNA transfections were also analyzed by flow cytometry which corroborated the confocal microscopy observations where higher pDNA fluorescence was noticed for GCL optimized formulations than Lipo2000*. The flow cytometry histograms depicting the pDNA cellular internalization using all the three GCL formulations in comparison with Lipo2000* are shown in Fig. S8 of ESI. This substantial pDNA cellular entry could be attributed to the observed excellent gene expressions using any of the three optimized lipoplexes.

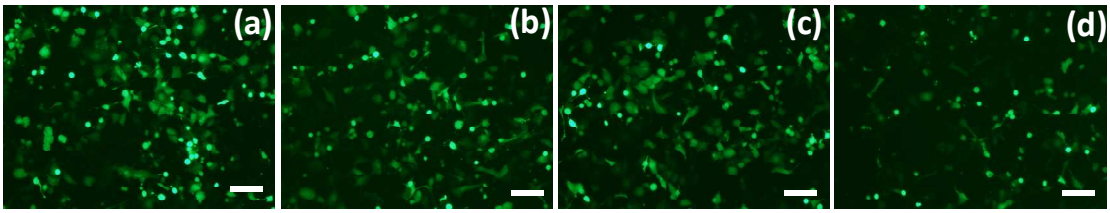

Fig. 8 Representative fluorescence microscopic images of GFP expression in HEK293T cells for transfections of pDNA (0.8 μg of pEGFP-C3) with $(C_{16}Im)_2(C_2O)$/DOPE (a), $(C_{16}Im)_2(C_2O)_2$/DOPE (b), and $(C_{16}Im)_2(C_2O)_3$/DOPE (c) in the presence of serum (+FBS). The optimized formulations (α = 0.2 at ρ_{eff} = 2.0) were used in transfections. Lipo2000* served as a positive control (d). Scale bar = 100 µm.

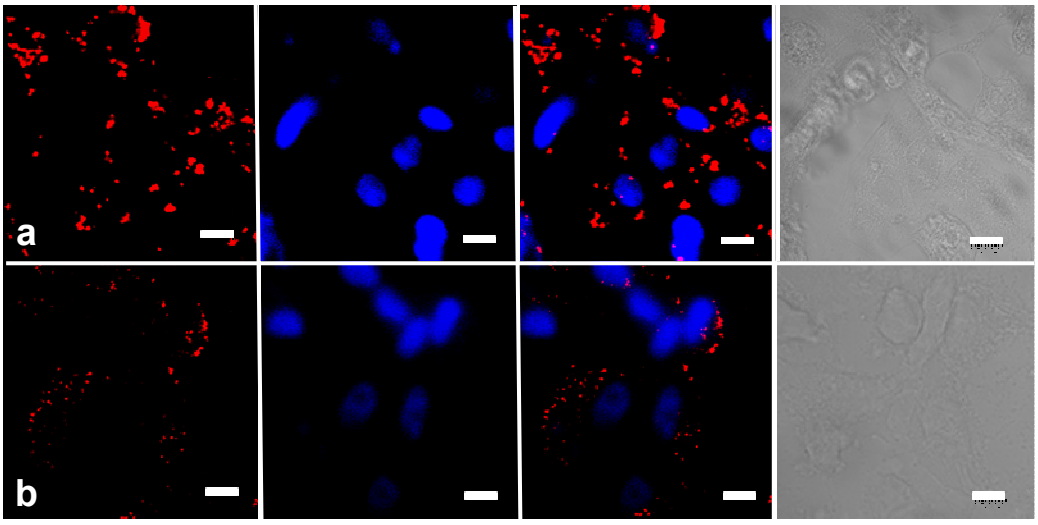

Fig. 9 Representative confocal microscopic images for Cy-5 labeled pDNA cellular internalization in HEK293T cells transfected by the optimized formulation (α = 0.2 at ρ_{eff} = 2.0) of the $(C_{16}Im)_2(C_2O)$/DOPE in the presence of serum (+FBS) (a) in comparison with Lipo2000* (b). The Cy5-labeled pDNA (1 μg) was used for transfection experiments. Panels (a and b) represent from left to right: pDNA fluorescence, DAPI stained nuclei, merge of previous two images and bright field images. Scale bar = 10 µm.

The reliability of cationic liposomal gene carriers for a practical application is associated with their non-toxic nature to a major extent while giving rise to significant gene expressions. Thus, biocompatible efficient liposomal gene carriers provide hope for successful gene therapy.[62] Fig. 10 reports the percentage of cell viability, obtained from the MTT assay, when the four cell lines were transfected with $(C_{16}Im)_2(C_2O)_n$/DOPE-pDNA lipoplexes of the optimum conditions (α = 0.2 and ρ_{eff} = 2.0). All these formulations did not report any obvious toxicity to any of the cell lines studied. Furthermore, the percentage of cell viability, observed after transfection, was considerably better than the commercial lipofection reagent, Lipo2000*.

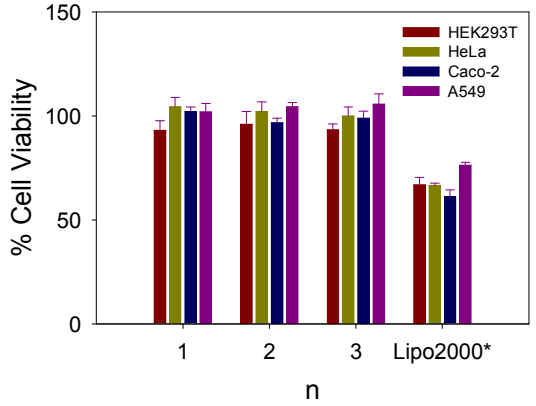

Fig. 10 Viabilities of four different cell lines transfected with $(C_{16}Im)_2(C_2O)_n$/DOPE-pDNA lipoplexes, using the optimized conditions (α = 0.2 at ρ_{eff} = 2.0) in the presence of serum (+FBS). Lipo2000* was used as a positive control.

3.3 Correlation between the structure of the lipoplex nano-aggregates and its biological activity

It is well-known that a gene delivery vector should show an efficient compaction, protection and efficient intracellular transport of pDNA for its expression. Based on the facts, it is evident that the structure of the lipoplex-type nano-aggregate is crucial for the desirable behaviour from gene transfection vectors and thus, the determination of the lipoplex structure in absence of cells has received particular attention from us.[22-25] The previous studies have concluded the following. Firstly, due to its fusogenic character with the cell membranes the transfection is favoured by the presence of a helper lipid as DOPE. The optimum transfection usually does not occur for the formulations at high content of the cationic lipid but when the GCL composition is moderate-to-low ($\alpha \leq 0.5$). Secondly, irrespective of the type of the cationic headgroups, TE is higher when the length of the spacer between the cationic heads is short or not so long and the coexistence of multiple structures in the lipoplex (i.e., lamellar + inverted hexagonal, or lamellar + lamellar) increases the transfection efficiency which points to a synergism effect. In order to stablish a correlation between the lipoplex structure and its biological activity several features have been observed from the biophysical and biological studies here. SAXS analysis has showed the coexistence of two lamellar structures in all compounds of the lipoplex series $(C_{16}Im)_2(C_2O)_n$/DOPE-pDNA with n = 1, 2, and 3, at low GCL composition (α = 0.2) i.e., at higher DOPE content, which is consistent with a higher transfection. The cryo-TEM micrographs indicate that the C-type structure present at low GCL composition (α = 0.2) is formed by less number of multilamellae (offering better possibilities to release pDNA) than the FP-type structure present at higher GCL composition ($\alpha \geq 0.5$). The coexistence of C-type and FP-type lamellar structures (observed by cryo-TEM but not from SAXS because their periodicity parameters are similar) is consistent with a moderate-to-high transfection efficiency for all the GCL series reported in this work, not only at α = 0.2 but also at moderate GCL composition ($\alpha \leq 0.5$). The high fluidity (low anisotropy levels) shown by the three $(C_{16}Am)_2(C_2O)_n$/DOPE-pDNA lipoplexes present them as flexible, fluid nano-aggregates potentially adequate as pDNA transfection vectors and the fluidity of the lipoplexes increases with the DOPE content (at α = 0.2) which is again consistent with the best TE observed at this GCL composition. Finally, the GCL with two imidazolium cationic headgroups having oligo-oxyethylene spacer of short-to-medium length results in lipoplex-type nano-aggregates for higher transfection efficiency and better biocompatibility, and thus they can be considered as the best series among those studied recently.

Taking all the observations together from gene transfection biology and cell viability measurements it could be concluded that the three gemini cationic lipids based on two imidazolium headgroups together an oligo-oxyethylene spacer of short-to-medium length bears the hope for successful *in vivo* applications and could be used straightforwardly.

4. Conclusions

A series of experiments consisting of a biophysical (electrochemistry, microscopy and structure) and biological studies for gene delivery (flow cytometry, fluorescence, confocal microscopy and cytotoxicity) have evidenced that mixed liposome nano-aggregates of DOPE and a gemini cationic lipid (GCL) with two cationic imidazolium groups separated by an oligo-oxyethylene spacer $[(C_{16}Im)_2(C_2O)_n$/DOPE] with n = 1, 2 or 3, compact and transfect pEGFP-C3 plasmid DNA significantly. The GCL composition (α) and the lipoplex effective charge ratio (ρ_{eff}) are shown to be important factors that determine their properties, structure and transfection efficiency. The three GCLs yield a lower effective charge ($q^+_{L^+}$ = +1.8) than its nominal one (+2), while pDNA is compacted yielding only a 25% effective negative charge (q^-_{pDNA} = -0.5 per bp). SAXS studies reveal the presence of two lamellar structures, one ($L_{\alpha,\ main}$) in the whole GCL composition, with periodicity (d) in the range 6.7-5.7 nm, and another one ($L_{\alpha\ DOPE\ rich}$) that coexists with the previous one at low GCL composition (α = 0.2), with a higher d values in the range 7.9-9.4 nm. The cryo-TEM analysis for the three $(C_{16}Im)_2(C_2O)_n$/DOPE-pDNA lipoplexes shows a multilamellar pattern consisting of series of cationic lipidic bilayers with pDNA sandwiched between them, with two types of lamellar packing: a cluster-type (C-type) and a fingerprint-type (FP-type), both with similar interlamellar spacing (d ~6.5 nm). This is in agreement with the $L_{\alpha,\ main}$ structure determined by SAXS. The C-type is observed alone at low α = 0.2, while the FP-type is present at moderate to high ($\alpha \geq 0.5$) values, although in the $(C_{16}Im)_2(C_2O)_2$/DOPE-pDNA lipoplex at α = 0.5 both lamellar patterns coexist. The *in vitro* transfection studies and cytotoxicity analysis reveal that the three lipoplex nano-aggregates reported in this work $[(C_{16}Im)_2(C_2O)_n$/DOPE-pDNA with n = 1, 2 or 3] are efficient gene transfection vectors even better than Lipo2000* and are also superior to previously studied lipoplexes containing other cationic headgroups or spacers. The optimum formulations in all the four cell lines are those with lower GCL composition (α = 0.2) and at low effective charge ratio (ρ_{eff} = 2.0) for cationic lipoplexes. Additionally, the length of the spacer in the GCL seems to have less importance in the present instance than in previous studies, although the $(C_{16}Im)_2(C_2O)_n$/DOPE-pDNA lipoplex with n = 1 or 3 shows slightly higher GFP expression than the formulation with n = 2. These features for the optimized formulations, have been attributed to the combination of several factors, as follows: (a) the fusogenic character of DOPE, which is predominant at α = 0.2, (b) the higher fluidity of the lipoplexes at α = 0.2 and at physiological temperature, (c) the coexistence of two lamellar structures at α = 0.2 that synergizes the TE of these lipid vectors, and (d) the higher biocompatibility of the GCLs reported in this work due the presence of both, two imidazolium cationic groups together with an oligo-oxyethylene spacer of short-to-medium length. In any case, all the optimum formulations reported here are highly efficient with negligible levels of toxicity, and thus, they may be

considered as promising gene transfection vectors for further biological applications.

Acknowledgements

Authors thank MECD of Spain (projects no. ACI2009-0867 and CTQ2012-30821), DST of India (project no. DST/INT/SPAIN/P-8/2009), and Univ. Complutense of Madrid (Spain) (project no. UCMA05-33-010). Authors also thank D. Hermida and BM26 at ESRF, Grenoble (France) for SAXS experiments, and E. Rossiynol and Servei de Microscopia of Univ. Autónoma of Barcelona (Spain) for cryo-TEM experiments.

Notes and references

Departments of [a]Organic Chemistry, and [d]Molecular Reproduction Development and Genetics, Indian Institute of Science, 560012 Bangalore, India

[b]Grupo de Química Coloidal y Supramolecular, Departamento de Química Física I, and [c]Departamento de Bioquímica y Biología Molecular I, Facultad de Ciencias Químicas, Universidad Complutense de Madrid, 28040 Madrid, Spain

[#]These authors contributed equally

*Authors to whom the correspondence should be addressed
S. Bhattacharya: Fax: +918023600529 e-mail: sb@orgchem.iisc.ernet.in
E. Aicart: Fax: +34913944135 e-mail: aicart@quim.ucm.es

[†]Electronic Supplementary Information (ESI) available: Details and tables of the effective charges for the three GCLs and plasmid DNA; SAXS diffractograms and parameters of the structures; ζ-potential plots; cryo-TEM images; fluorescence anisotropy results; transfection efficiency and cell viability results in absence (-FBS) and presence (+FBS) of serum in four cell lines; and fluorescence microscopy images of the *in vitro* transfected Caco-2 and HeLa cells.

1 R. S. Dias and B. Lindman, *DNA Interaction with Polymers and Surfactants*, Wiley & Sons, Hoboken, 2008.
2 D. D. Lasic, *Liposomes in Gene Delivery*, CRC Press, Boca Raton, FL, 1997.
3 G. Caracciolo and H. Amenitsch, *Eur. Biophys. J.*, 2012, **41**, 815-829.
4 J. H. Felgner, R. Kumar, C. N. Sridhar, C. J. Wheeler, Y. T. Tsai, R. Border, P. Ramsey, Martin and P. L. Felgner, *J. Biol. Chem.*, 1993, **269**, 2550-2561.
5 C. R. Safinya, K. Ewert, A. Ahmad, H. M. Evans, U. Raviv, D. J. Needleman, A. J. Lin, N. L. Slack, C. George and C. E. Samuel, *Philos. Trans. R. Soc., A*, 2006, **364**, 2573-2596.
6 S. Bhattacharya and A. Bajaj, *Chem. Commun.*, 2009, 4632-4656.
7 I. M. Verma and M. D. Weitzman, *Annu. Rev. Biochem.*, 2005, **74**, 711-738.
8 I. M. Verma and N. Somia, *Nature*, 1997, **389**, 239-242.
9 R. I. Zhdanov, O. V. Podobed and V. V. Vlassov, *Bioelectrochemistry*, 2002, **58**, 53-64.
10 H. Amenitsch, G. Caracciolo, P. Foglia, V. Fuscoletti, P. Giansanti, C. Marianecci, D. Pozzi and A. Lagana, *Colloids Surf. B*, 2011, **82**, 141-146.
11 R. Koynova and B. Tenchov, *Soft Matter*, 2009, **5**, 3187-3200.
12 C. Marchini, D. Pozzi, M. Montani, C. Alfonsi, A. Amici, H. Amenitsch, S. C. De Sanctis and G. Caracciolo, *Langmuir*, 2010, **26**, 13867-13873.
13 A. Kulkarni, R. VerHeul, K. DeFrees, C. J. Collins, R. A. Schuldt, A. Vlahu and D. H. Thompson, *Biomaterials Science*, 2013, **1**, 1029-1033.
14 M. Donkuru, I. Badea, S. Wettig, R. Verrall, M. Elsabahy and M. Foldvari, *Nanomedicine*, 2010, **5**, 1103-1127.
15 M. Kapoor, D. J. Burgess and S. D. Patil, *Int. J. Pharm.*, 2012, **427**, 35-57.
16 R. Zana, *Adv. Colloid Interface Sci.*, 2002, **97**, 205-253.
17 A. J. Kirby, P. Camilleri, J. Engberts, M. C. Feiters, R. J. M. Nolte, O. Soderman, M. Bergsma, P. C. Bell, M. L. Fielden, C. L. G. Rodriguez, P. Guedat, A. Kremer, C. McGregor, C. Perrin, G. Ronsin and M. C. P. van Eijk, *Angew. Chem. Int. Ed.*, 2003, **42**, 1448-1457.
18 F. M. Menger and J. S. Keiper, *Angew. Chem. Int. Ed.*, 2000, **39**, 1906-1920.
19 A. Bajaj, P. Kondiah and S. Bhattacharya, *J. Med. Chem.*, 2007, **50**, 2432-2442.
20 A. Bajaj, P. Kondaiah and S. Bhattacharya, *Bioconjugate Chem.*, 2007, **18**, 1537-1546.
21 A. Bajaj, P. Kondaiah and S. Bhattacharya, *Biomacromolecules*, 2008, **9**, 991-999.
22 A. L. Barran-Berdon, S. K. Misra, S. Datta, M. Muñoz-Ubeda, P. Kondaiah, E. Junquera, S. Bhattacharya and E. Aicart, *J. Mat. Chem. B*, 2014, **2**, 4640-4652.
23 S. K. Misra, M. Muñoz-Ubeda, S. Data, A. L. Barran-Berdon, C. Aicart-Ramos, P. Castro-Hartmann, P. Kondaiah, E. Junquera, S. Bhattacharya and E. Aicart, *Biomacromolecules*, 2013, **14**, 3951-3963.
24 M. Muñoz-Ubeda, S. K. Misra, A. L. Barran-Berdon, C. Aicart-Ramos, M. B. Sierra, J. Biswas, P. Kondaiah, E. Junquera, S. Bhattacharya and E. Aicart, *J. Am. Chem. Soc.*, 2011, **133**, 18014-18017.
25 M. Muñoz-Ubeda, S. K. Misra, A. L. Barran-Berdon, S. Data, C. Aicart-Ramos, P. Castro-Hartmann, P. Kondaiah, E. Junquera, S. Bhattacharya and E. Aicart, *Biomacromolecules*, 2012, **13**, 3926-3937.
26 C. Bombelli, F. Faggioli, P. Luciani, G. Mancini and M. G. Sacco, *J. Med. Chem.*, 2007, **50**, 6274-6278.
27 Z. Pietralik, R. Krzyszton, W. Kida, W. Andrzejewska and M. Kozak, *Int. J. Mol. Sci.*, 2013, **14**, 7642-7659.
28 V. D. Sharma, J. Lees, N. E. Hoffman, E. Brailoiu, M. Madesh, S. L. Wunder and M. A. Ilies, *Molec. Pharm.*, 2014, **11**, 545-559.
29 V. D. Sharma and M. A. Ilies, *Med Res Rev*, 2014, **34**, 1-44.
30 P. Luciani, C. Bombelli, M. Colone, L. Giansanti, S. J. Ryhanen, V. M. J. Saily, G. Mancini and P. K. J. Kinnunen, *Biomacromolecules*, 2007, **8**, 1999-2003.
31 S. D. Wettig, R. E. Verrall and M. Foldvari, *Curr. Gene Ther.*, 2008, **8**, 9-23.
32 G. L. Zhen, T. M. Hinton, B. W. Muir, S. N. Shi, M. Tizard, K. M. McLean, P. G. Hartley and P. Gunatillake, *Molec. Pharm.*, 2012, **9**, 2450-2457.
33 D. F. Zhi, S. B. Zhang, B. Wang, Y. N. Zhao, B. L. Yang and S. J. Yu, *Bioconjugate Chem.*, 2010, **21**, 563-577.
34 T. Zhou, A. Llizo, P. Li, C. Z. Wang, Y. Guo, M. Q. Ao, L. Bai, Y. Yang and G. Xu, *J. Phys. Chem. B*, 2013, **117**, 26573-26581.
35 S. De, V. K. Aswal, P. S. Goyal and S. Bhattacharya, *J. Phys. Chem. B*, 1998, 6152-6160.
36 D. Zhi, S. Zhang, S. Cui, Y. Zhao, Y. Wang and D. Zhao, *Bioconjugate Chem.*, 2013, **24**, 487-519.
37 S. Datta, J. Biswas and S. Bhattacharya, *J. Colloid Interface Sci.*, 2014, **430**, 85-92.
38 A. Pal, S. Datta, V. K. Aswal and S. Bhattacharya, *J. Phys. Chem. B*, 2012, **116**, 13239-13247.
39 A. Rodriguez-Pulido, F. Ortega, O. Llorca, E. Aicart and E. Junquera, *J. Phys. Chem. B*, 2008, **112**, 12555-12565.
40 J. Dubochet, M. Adrian, J. J. Chang, J. C. Homo, J. Lepault, A. W. McDowall and P. Schultz, *Q. Rev. Biophys.*, 1988, **21**, 129-228.
41 J. Bednar and C. L. Woodcock, *In Chromatin*, Academic Press Inc., San Diego, 1999.
42 J. Dubochet, B. Zuber, M. Eltsov, C. Bouchet-Marquis, A. Al-Amoudi and F. Livolant, in *Cellular Electron Microscopy*, 2007, pp. 385-406.
43 A. Rodriguez-Pulido, E. Aicart and E. Junquera, *Langmuir*, 2009, **25**, 4402-4411.
44 M. B. Hansen, S. E. Nielsen and K. Berg, *J. Immunol. Methods*, 1989, **119**, 203-210.
45 K. Ewert, N. L. Slack, A. Ahmad, H. M. Evans, A. J. Lin, C. E. Samuel and C. R. Safinya, *Curr. Med. Chem.*, 2004, **11**, 133-149.

46 A. L. Barran-Berdon, M. Muñoz-Ubeda, C. Aicart-Ramos, L. Perez, M. R. Infante, P. Castro-Hartmann, A. Martin-Molina, E. Aicart and E. Junquera, *Soft Matter*, 2012, **8**, 7368-7380.
47 A. Rodriguez-Pulido, E. Aicart, O. Llorca and E. Junquera, *J. Phys. Chem. B*, 2008, **112**, 2187-2197.
48 Y. Han and Y. Wang, *Phys. Chem. Chem. Phys.*, 2011, **13**, 1939-1956.
49 X. Wang, J. Wang, Y. Wang, H. Yan, P. Li and R. K. Thomas, *Langmuir*, 2004, **20**, 53-56.
50 I. Koltover, T. Salditt and C. R. Safinya, *Biophys. J.*, 1999, **77**, 915-924.
51 G. Caracciolo, D. Pozzi, A. Amici and H. Amenitsch, *J. Phys. Chem. B*, 2010, **114**, 2028-2032.
52 C. L. Pizzey, C. M. Jewell, M. E. Hays, D. M. Lynn, N. L. Abbott, Y. Kondo, S. Golan and Y. Tahnon, *J. Phys. Chem. B*, 2008, **112**, 5849-5857.
53 S. Huebner, B. J. Battersby, R. Grimm and G. Cevc, *Biophys. J.*, 1999, **76**, 3158-3166.
54 Y. S. Tarahovsky, V. A. Rakhmanova, R. M. Epand and R. C. MacDonald, *Biophys. J.*, 2002, **82**, 264-273.
55 M. Rosa, M. D. Miguel and B. Lindman, *J. Colloid Interface Sci.*, 2007, **312**, 87-97.
56 S. Bhattacharya and S. S. Mandal, *Biochemistry*, 1998, **37**, 7764-7777.
57 A. Aljaberi, M. Spelios, M. Kearns, B. Selvi and M. Savva, *Colloids Surf. B*, 2007, **57**, 108-117.
58 R. Zantl, L. Baicu, F. Artzner, I. Sprenger, G. Rapp and J. O. Rädler, *J. Phys. Chem. B*, 1999, **103**, 10300-10310.
59 A. Rodriguez-Pulido, A. Martin-Molina, C. Rodriguez-Beas, O. Llorca, E. Aicart and E. Junquera, *J. Phys. Chem. B*, 2009, **113**, 15648-15661.
60 O. Zelphati, L. S. Uyechi, L. G. Barron and F. C. Szoka Jr, *Biochim. Biophys. Acta*, 1998, **1390**, 119-133.
61 I. S. Zuhorn, J. Visser, U. Bakowsky, J. B. F. N. Engberts and D. Hoekstra, *Biochim. Biophys. Acta*, 2002, **1560**, 25-36.
62 H. T. Lv, S. B. Zhang, B. Wang, S. H. Cui and J. Yan, *J. Control. Release*, 2006, **114**, 100-109.